

Supplemental Online Material

Materials and Methods

Antibodies and reagents:

The following antibodies were obtained from commercial sources: STAT3, pSTAT3 (Y705), pSTAT3 (S727), Akt, pAkt, Bcl-X (Cell Signaling, Beverly, MA); Tubulin (Sigma, St. Louis, MO); H-Ras, Erk1/2, pErk1/2, RalA, F1-ATPase, and IGF1R α (Santa Cruz Biotechnology, Santa Cruz, CA). All other reagents were purchased from Fisher Scientific (Pittsburg, PA), except as noted.

Cloning and expression plasmids:

The expression construct for v-Src was generated by subcloning from pMv-Src into pBabePuro to generate pBabePuro-v-Src. The retroviral constructs expressing H-RasV12 (pBabePuro-H-RasV12), N-RasV12 (pBabePuro-N-RasV12) and K-RasV12 (pBabePuro-K-RasC12) were the kind gift of A. Pellicer. Retroviral (pBabe-GFP) constructs expressing wild type STAT3, and the STAT3 mutants Y705F, DNA binding domain (DBD), SH2 domain (SH2) and S727A have been previously described (S1). Retroviral (pBabe-GFP) constructs expressing STAT3 β and Δ 132 STAT3 were gifts from R. Jove and S. Watowich, respectively. Retroviral (pBabe-GFP) constructs expressing STAT3 S727D and nuclear localization site I, II and III mutations were generated by site-directed mutagenesis using the following primers:

(S727D) GCAATACCATTGACCTGCCCATGGACCCCCGCACTTTAGATT

(NLSI) CTCACAATGCTTGCCGCCATCTGCTCGAGGGCTGTGAGC

(NLS II) GCACCTGACCCTTGCGGAGCAGGCATGTGGGAATGGAGG

NLS III was generated by sequentially mutating both NLS I and II. Retrovirus expressing (pBabe GFP) RalA and Ral mutants (RalA-28N and RalA72L) were obtained from L. Feig. The retroviral constructs (pBabe-puro) expressing H-RasV12 mutants H-RasV12/35S, H-RasV12/37G and H-RasV12/40C, B-Raf 600E mutant, p100-CAAX and RLF-CAAX were kind gifts from C. Der. Retroviruses (MSCV-GFP) expressing wild

type STAT3, STAT3-Y705F or STAT3-S727A fused to an N-terminal mitochondrial targeting sequence from cytochrome c oxidase subunit VIII were constructed by standard procedures. The retroviral constructs (pSuper-Retro) for hairpin RNA (shRNA) against H-Ras and scrambled control were obtained from M. Philips. The sequence of the sense strand of the H-Ras shRNA is:

5'-gatccccACGGGTGAAGGACTCGGATttcaagagaATCCGAGTCCTTCACCCGTttttggaa-3'

where the 19-nucleotide H-Ras targetting sequence is capitalized. The retroviral constructs (pSuper-Retro) for hairpin RNA (shRNA) against human STAT3 and scrambled control have been described (S2). Hairpin constructs were stably introduced into cells, selected, and expanded as pools, and the efficiency of knockdown was determined by western blotting.

Cell Culture:

Immortalized STAT3-deficient mouse embryo fibroblasts were generated as described previously (S1) and STAT3 deletion was confirmed by genomic PCR and immunoblotting. Wild type STAT3 or STAT3 mutants (Y705F, S727A, S727D, SH2, DBD, NLS, Δ 132, MTS-STAT3-WT, MTS-STAT3-Y705F or MTS-STAT3-S727A) were stably introduced using retroviruses, as was stable expression of the oncogenes v-Src, H-RasV12, N-RasV12, and K-RasV12. Transduced cell lines were obtained as pools of either drug-resistant cells or sorted GFP-positive cells, depending on the vector used, and the levels of expression of the transduced genes were determined by immunoblotting. All cell lines were grown in DMEM supplemented with 5% CS in a humidified incubator at 37°C and 5 % CO₂, except MCF10A cells, which were cultured in DMEM:F12 50:50 mix supplemented with 20ng/mL EGF, 100ng/mL cholera toxin, 0.01mg/mL insulin, 72.5 ng/mL hydrocortisone, and 5% horse serum.

Glucose starvation:

1x10⁵ cells were plated per well in 6 well plates in complete medium. Once cells adhered to the plate, medium was replaced with DMEM containing high glucose (4.5g/L) or low glucose (0.5g/L) and cultured in 5% CO₂ with either normal air (~20% oxygen) or reduced oxygen (2%) in a humidified incubator at 37° C for 72 h. Cells were collected

and the proportion of apoptotic cells calculated by trypan blue exclusion assay.

Soft agar assay:

Cells (1×10^4) were seeded in 0.35% low-melting agarose, prepared in standard growth medium. Cells were cultured in a humidified incubator at 37°C and 5% CO₂ for 14-21 d and colonies greater than 0.2 mm² were scored as average colony number from three biological replicas. Multiple, independent cell pools of Ras-expressing wild type, STAT3-null, and STAT3-reconstituted cells gave analogous results.

Subcutaneous tumor assay:

BALB/c^{-nu/nu} mice or Fox Chase SCID mice (Taconic Lab, Germantown, NY) were injected with 100 mg/kg cyclophosphamide diluted in PBS 3 d prior to inoculation with 1×10^4 tumor cells. Tumor growth was observed every 3 to 4 d, and average tumor volume was calculated from cohorts of 5 mice/group.

Cell fractionation and purification of mitochondria:

Mitochondria were isolated by using differential centrifugation following mechanical cell disruption. 10^8 cells were harvested by centrifugation, washed once with cold PBS, and resuspended in 10 volumes of ice-cold buffer A (220mM sorbitol, 70mM sucrose, 50mM MOPS pH 7.4, 1mM EDTA, supplemented with protease inhibitors). Cells were dounce homogenized and unbroken cells and nuclei were removed by centrifugation at 800g for 10 min at 4°C twice. To isolate crude mitochondrial fractions, supernatants were further centrifuged at 7800g for 10 min at 4°C. The mitochondria were washed once in buffer A and resuspended in buffer B (250mM sucrose, 1mM EDTA, 10mM Tris-HCl pH7.4, supplemented with protease inhibitors). Mitochondria were further purified by centrifugation in a self-forming 2.5 M sucrose-percoll gradient at 60,000g for 45 min at 4°C. The mitochondria were collected and washed twice in buffer B at 7800g for 10 min at 4°C. Organelle-free supernatant and plasma membrane fractions were prepared by centrifugation of supernatants following crude mitochondrial preparations at 100,000g for 2 h at 4°C. The supernatant was collected as the S100 (organelle-free cytosol) fraction and the plasma membrane pellet was washed in buffer B and centrifuged at 100,000g for

2 h at 4°C. This pellet was collected as the P100 (plasma membrane) fraction. Cytosolic and nuclear fractions were isolated as previously described (S3). Protein concentrations were determined using the Bradford protein assay (Biorad) and fraction purities were verified by immunoblotting.

***In vitro* cell death assays:**

Cells (10^5) were incubated in the presence of either vehicle or the indicated compounds at the indicated concentrations for 24 h. Cell viability was measured by trypan blue exclusion.

Ral activity assay:

GST-RalBP1 expression was induced by treating pGEX2T-RalBP-1 expressing *E. coli* with IPTG (final concentration of 0.1mM) for 3 h at 37°C. Cells were collected by centrifugation at 3000g for 10 min at 4°C, resuspended in PBS supplemented with 0.5 mM DTT and protease inhibitor cocktail (Sigma, St. Louis, MO) and lysed by sonication. Triton X-100 was added to the sonicated cells to a final concentration of 1% and incubated at 4°C for 15 min with gentle agitation. The sample was passed through an 18 gauge needle and cell debris was cleared by centrifugation at 12000g for 10 min at 4°C. GST-fusion proteins were collected with glutathione-Sepharose beads (Sigma, St. Louis, MO) as recommended by the manufacturer. Purified GST-fusion proteins were equilibrated in RBD buffer (50 mM Tris pH 7.5, 200 mM NaCl, 2.5 mM MgCl₂, 2 mM orthovanadate, 1% v/v NP-40, 10% glycerol, 20 mM NaF, and protease inhibitor cocktail (Sigma, St. Louis, MO)), combined with 1.5mg of cellular protein, and incubated overnight at 4°C with gentle agitation. Beads were washed three times in RBD buffer, and following the final wash beads were boiled in Laemmli SDS-loading buffer. Eluted proteins were separated by SDS-PAGE and analyzed by western blotting with an antibody specific for RalA.

Immunoblot analysis:

Protein preparations were resolved on 10% SDS-PAGE gels, transferred to PVDF membranes (Millipore), and the membranes were incubated for 1 hour in 5% non-fat milk

powder in TBS (20 mM Tris-HCl pH 7.5, 150 mM NaCl). Blots were probed with primary antibodies diluted in TBS-0.1% Tween-20 buffer overnight at 4°C. The blots were washed four times and incubated with 1:15,000 dilution of infrared fluor-conjugated secondary antibody (Li-Cor) and scanned using an Odyssey infrared scanner (Li-Cor).

Quantitative real time PCR:

RNA was isolated from purified mitochondria by Trizol (Invitrogen) according to manufacturer's protocol and reverse transcribed into cDNA. Mitochondrial DNA was isolated from purified mitochondria by incubating mitochondrial pellets in 50 mM NaOH for 1hr followed by the addition of Tris pH 7.4 to a final concentration of 130 mM. Sybr green-based real time PCR was performed using the following primers to analyze mitochondrial mRNA or DNA:

NADH subunit 1 (ND1): F 5'CCGGCCCATTCGCGTTATTCTTTA and R 5'-AAGCGTGGATAGGATGCTCGGATT; NADH subunit 2 (ND2): F 5'-TAACTCAAGGGATCCCCTGCACA and R 5'-TGGTTAAGTCCTCCTCATGCTCCT; NADH subunit 3 (ND3) F 5'-TGCGGATTTGACCCTACAAGCTCT and R 5'-CATGGTAGTGGAAGTAGAAGGGCA; NADH subunit 4 (ND4): F 5'-ACATGGCCTCACATCATCACTCCT and R 5'-AGATCATTTGAAGTCCTCGGGCCA; NADH subunit 5 (ND5): F 5'-TACTGCAGCCCTACAAGCAATCCT and R 5'-GGTGGAGGCCAAATTGTGCTGATT; NADH subunit 6 (ND6): F 5'-CAGTGGCCATAGCAGTCGTATATC and R 5'-GGTTGGTTGTCTTGGGTTGGCATT; NADH subunit 4L (ND4L): F 5'-ATCCACATTGCTATGCCTGGAAGG and R 5'-GGACGTAATCTGTTCCGTACGTGT; Cytochrome B (CytB): F 5'-ATTCCTTCATGTCGGACGAGGCTT and R 5'-TGGGATGGCTGATAGGAGGTTTGT; Cytochrome C oxidase subunit 1 (CytC1): F 5'-ACTTGCAACCCTACACGGAGGTAA and R 5'-TCGTGAAGCACGATGTCAAGGGAT; Cytochrome C oxidase subunit 2 (CytC2): F 5'-ACCTGGTGAACCTACGACTGCTAGA and R 5'-

TCCTGGTCGGTTTGATGCTACTGT; Cytochrome C oxidase subunit 3 (CytC3): F 5'-
TAACCCTTGGCCTGCTACCAATA and R 5'-
AATAGGAGTGTGGTGGCCTTGGTA; ATP synthase Fo subunit 6 (ATP6): F 5'-
ATGGCATTAGCAGTCCGGCTTACA and R 5'-
TGTAATGGTAGCTGTTGGTGGGCT; ATP synthase Fo subunit 8 (ATP8): F 5'-
TGCCACAACACTAGATACATCAACATGA and R 5'-
TGGTGAAGGTGCTAGTGGGAATGT.

FACS (Mitotracker Red and TMRE):

10^6 cells were incubated with 50 nM Mitotracker Red (Molecular Probes) for 30 min at 37°C. Cells were removed from plates with trypsin, washed twice and resuspended in PBS at a concentration of 5×10^6 cells/mL. Mitotracker Red fluorescence emission was measured in the far-red channel following excitation by a 488 nm laser on a Beckman Coulter Cytomics FC500 cytometer.

For $\Delta\psi_m$ measurements, cells were incubated for 20 min at 37°C in media containing 50 nM TMRE. TMRE fluorescence was detected in the far-red channel following excitation by a 488nm laser and detection with an FL-2 bandpass filter on a Beckman Coulter Cytomics FC500 cytometer.

Lactate Dehydrogenase (LDH) Activity: 10^5 cells were disrupted by dounce homogenization in PBS, and LDH activity was determined using VITROS LDH slides as per manufacturer's instructions.

Measurement of individual electron transport chain (ETC) complex activity: ETC activity was measured on purified mitochondria from H-RasV12-expressing wild type or STAT3-deficient cells following solubilization in 0.1 M phosphate buffer (pH7.2) and 1% cholate. Complex I NADH:duroquinone oxidoreductase; Complex II Succinate:2,6-dichlorphenol (DCIP) oxidoreductase; Complex III Ubiquinol:ferricytochrome C oxidoreductase; Complex IV Ferrocytochrome C: oxygen oxidoreductase and Complex V ATPase activities were measured as previously described (S4-8). Citrate synthase activity

was used as a control for equivalent mitochondrial numbers and integrity in ETC assays and was measured as previously described (S9).

Measurement of total cellular ATP concentration: ATP concentrations were determined using the Cell Titer Glo™ kit (Promega, Madison, WI) as per manufacturer's instructions.

Supplemental Text

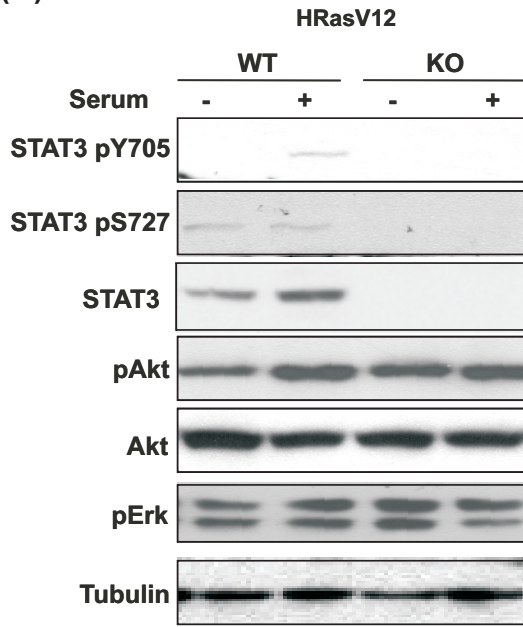
Activated Ras signals primarily through stimulation of the MAPK, PI3K, and RalGDS pathways (S10). Given the apparent lack of a nuclear function of STAT3 during Ras transformation, we probed effects of STAT3 on cytoplasmic Ras signaling. We examined the phosphorylation state of Erk1/2 and Akt as markers of the activity of the MAPK and PI3K pathways respectively (fig. S1A). To assay the activity of the RalGDS pathway, we determined the STAT3-dependence of Ral activation as measured by the levels of GTP-bound RalA (fig. S3A). Analysis of STAT3 phosphorylation revealed that Ras activation drives phosphorylation on S727 but not tyrosine 705. As expected, serum stimulation resulted in STAT3 tyrosine and serine phosphorylation. While Akt and Erk were phosphorylated in Ras-transformed cells, this phosphorylation was not altered by the absence of STAT3, indicating that Ras-mediated activation of the Raf/MEK/ERK and PI3K pathways are STAT3-independent. In contrast, Ras-induced activation of RalA was dependent on STAT3 (fig. S3A). To determine the role of RalA activity in Ras-mediated transformation, we generated cell lines that expressed constitutively active (72L) or dominant negative (28N) RalA mutations. However, expression of constitutively activated RalA could not compensate for the loss of STAT3 and expression of Ral28N did not diminish Ras-mediated transformation in STAT3-expressing cells (fig. S3B). Therefore, while Ras-mediated activation of RalA was dependent on STAT3, this pathway alone did not appear to explain the STAT3-dependence of Ras-mediated transformation.

We also queried the role of STAT3 in Ras signaling genetically using Ras effector

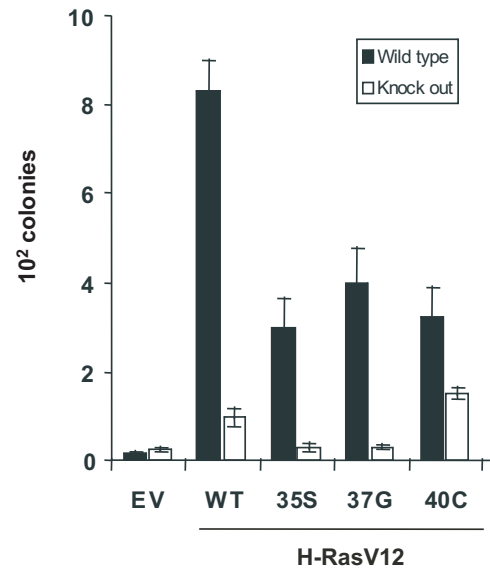
domain mutants that selectively activate single downstream pathways (S10). These mutant H-Ras proteins contain the activating V12 mutation in combination with a second mutation within the effector domain (residues 32-40) that interacts with downstream effector proteins, thereby limiting signaling to individual effector pathways: T35S impairs PI3K and RalGDS but not Raf activation; E37G prevents Raf and PI3K signaling but not RalGDS activation; and Y40C targets PI3K signaling but not Raf or RalGDS. Colony formation assays showed that optimal anchorage independent growth required cooperation of more than one Ras effector pathway (fig. S1B). While activation of a single downstream pathway was sufficient to support a modest level of anchorage independent growth, colony formation remained STAT3 dependent. Interestingly, absence of STAT3 was less detrimental to the colony forming capacity of cells transformed with H-RasV12/40C, suggesting that the PI3K pathway is a less STAT3-dependent arm of the Ras-activated signaling cascade. In contrast, selective activation of the MAPK and Ral pathways by the 35S and 37G mutants led to complete dependence on STAT3 for anchorage-independent growth. To confirm that there is no single Ras-activated cytosolic signaling pathway that is necessary for transformation in the context of STAT3, we generated cell lines expressing constitutively active Ras effectors and measured anchorage-independent growth (fig. S1C). No single activated signaling pathway potently stimulated anchorage independent growth, and B-Raf-600E (MAPK activator) and Rlf-CAAX (Ral activator) showed clear dependence on STAT3 for transformation. Constitutively active PI3K (p110-CAAX), consistent with the results obtained with mutant Ras alleles, was less STAT3-dependent. Combined activation of MAPK and PI3K pathways by co-expression of B-Raf-600E and p110-CAAX largely compensated for the absence of oncogenic Ras, consistent with a minor role for activated Ral in mouse cell transformation (S11). However, these activating alleles had little transforming capacity in the absence of STAT3, reinforcing the notion that there are multiple Ras-activated mechanisms required for transformation, of which STAT3 is an essential arm. These data confirm that while STAT3 is essential for H-Ras-transformation, it is independent, parallel, or downstream of the common Ras-activated pathways and functions from the cytoplasm.

Figure S1

(A)



(B)



(C)

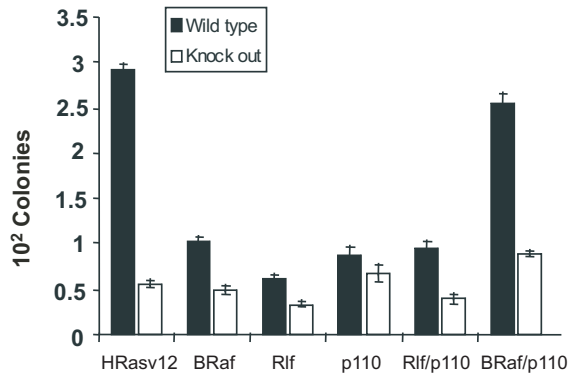


Figure S2

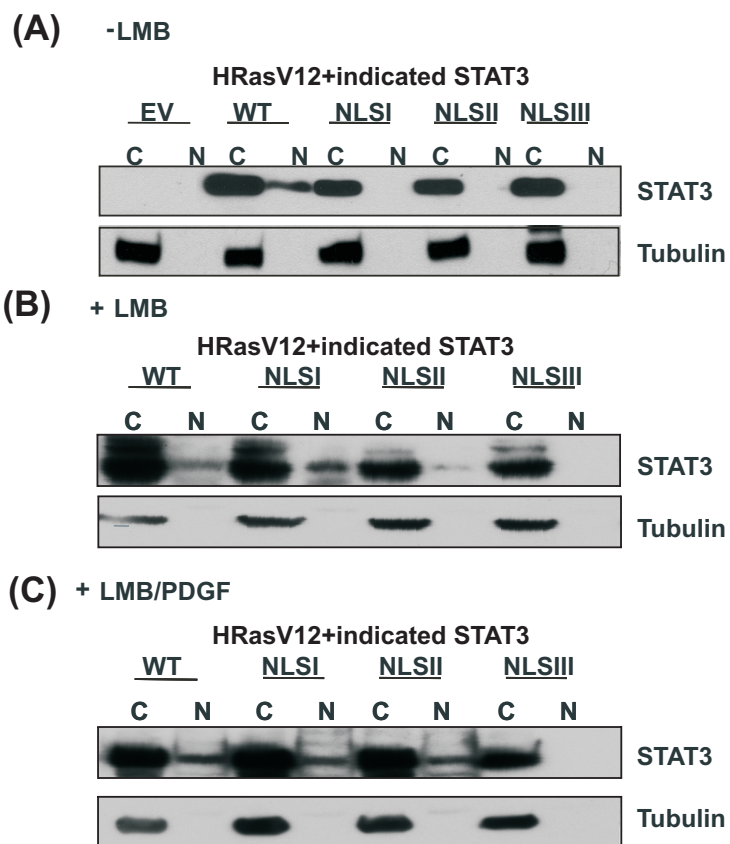
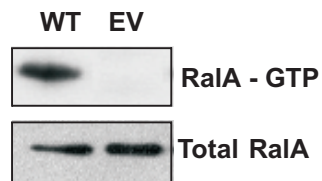


Figure S3

(A)

HRasV12+indicated STAT3



(B)

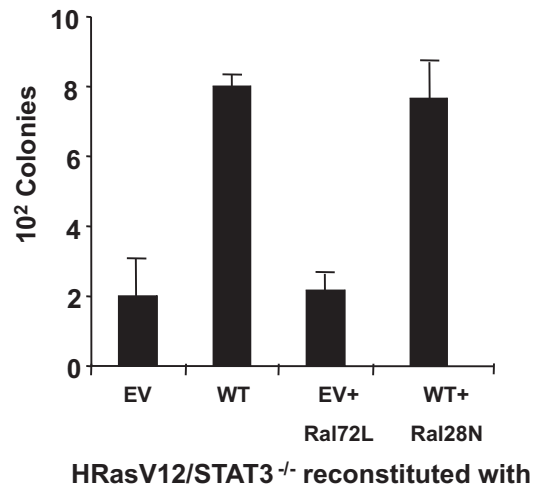
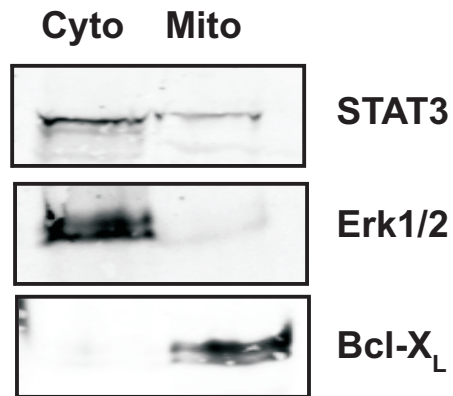


Figure S4

(A)



(B)

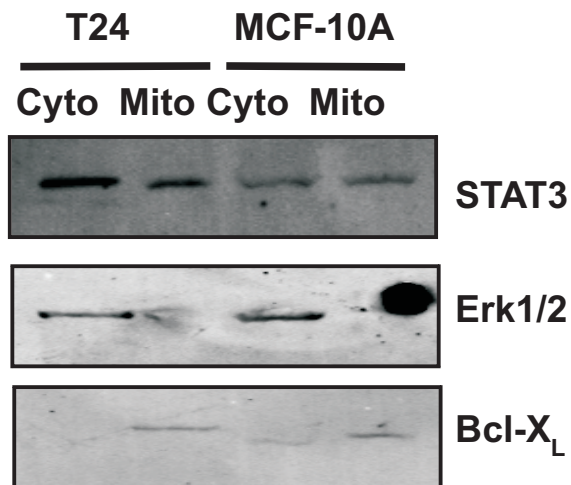
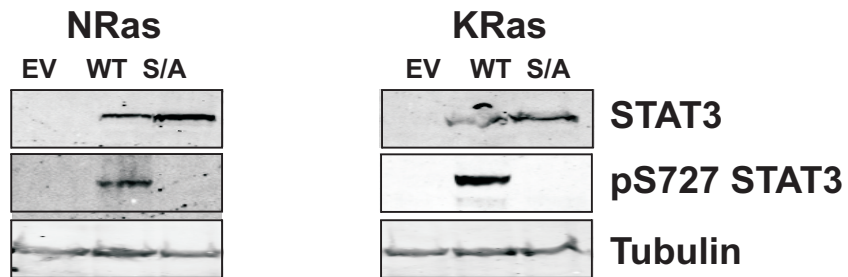


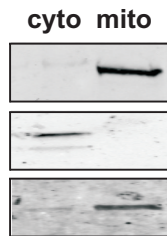
Figure S5

(A)



(B)

NRas MTS-STAT3



KRas MTS-STAT3

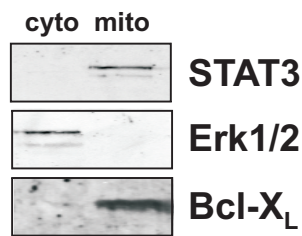
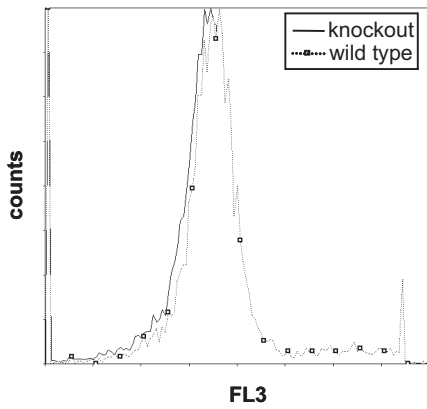
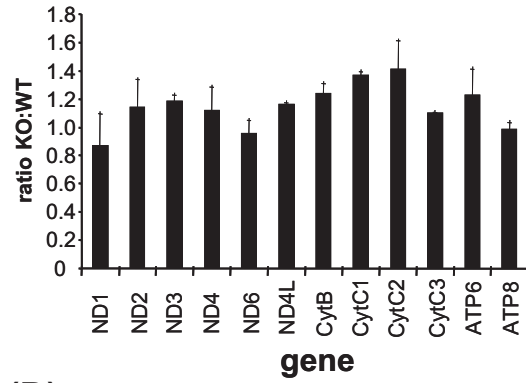


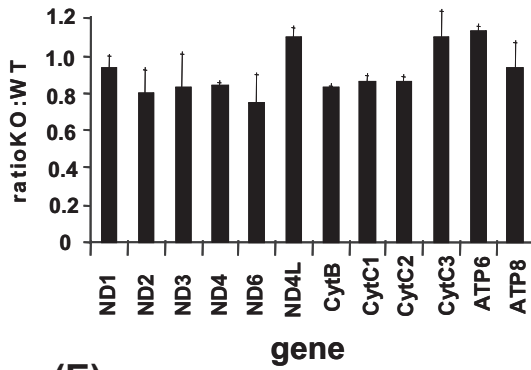
Figure S6
(A)



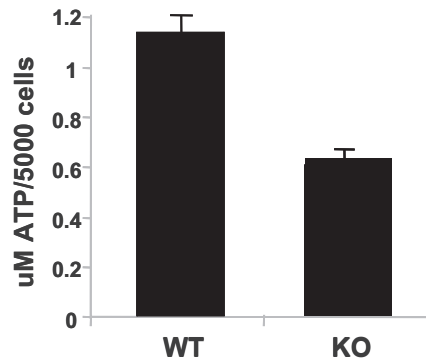
(B)



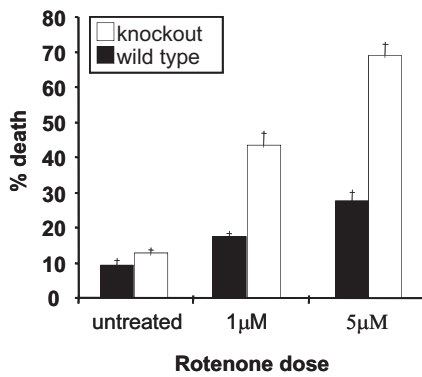
(C)



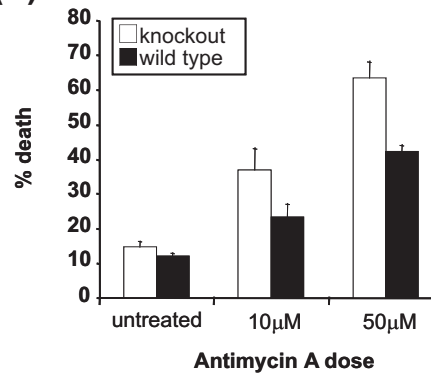
(D)



(E)



(F)



(G)

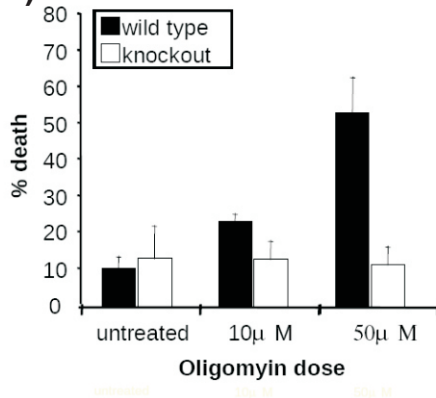
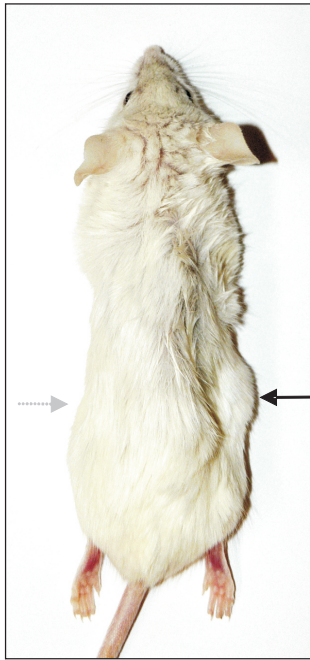
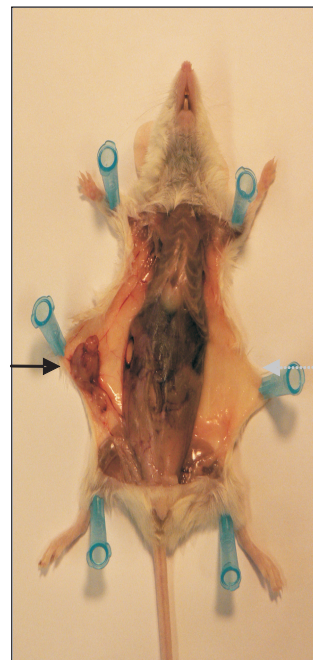


Figure S7

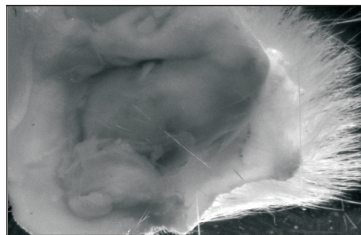
(A)



(B)



(C)



(D)

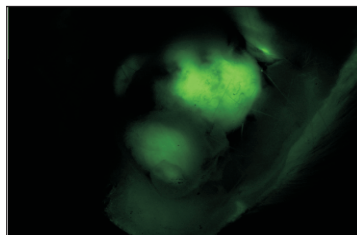
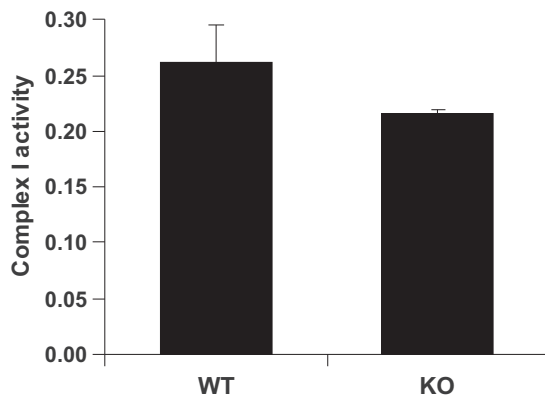
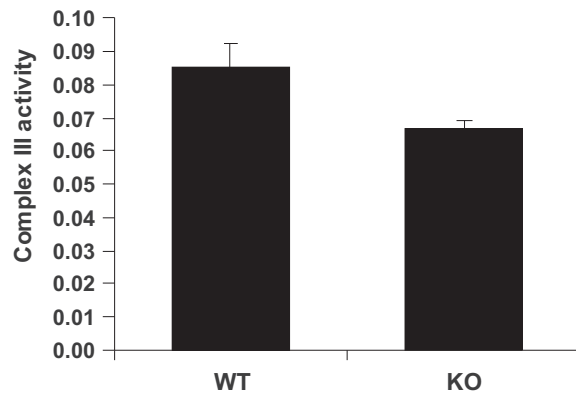


Figure S8

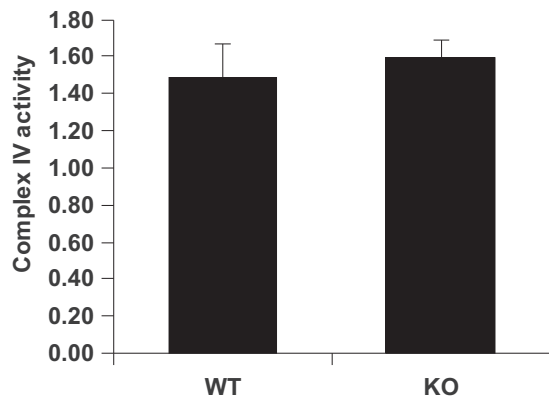
(A)



(B)



(C)



Supplemental Figure Legends

Figure S1: Ras-activated signaling pathways are independent of STAT3. (A) Protein extracts from wild type (WT) or STAT3-deficient (KO) cells expressing H-RasV12 were analyzed by immunoblotting with antibodies specific to the phosphorylated forms of STAT3 (pY705 and pS727), Akt (pAkt), and Erk1/2 (pErk), as well as total STAT3, Akt, and tubulin to serve as loading controls. Serum treatment provided a positive control for phosphorylation. (B) Wild type (filled bars) or STAT3-deficient cells (open bars) transduced with activated H-Ras and H-Ras mutants selectively activating the MAPK pathway (35S), the Ral pathway (37G), or the PI3-K pathway (40C) were analyzed for soft agar colony formation. Average colony number was calculated from three biological replicates. Error bars represent SD. (C) Wild type (filled bars) or STAT3-deficient cells (open bars) transduced with H-RasV12 or constitutively-activated downstream mediators of Ras signaling. B-Raf, Rlf, p110, or a combination of B-Raf/p110 were analyzed for soft agar colony formation. Average colony number was calculated from three biological replicates. Error bars represent SD.

Figure S2: Mutation of both nuclear localization sequences is necessary to restrict STAT3 to the cytoplasm. STAT3-deficient cells expressing H-RasV12 were stably transduced with empty vector (EV), wild type STAT3 (WT), or versions of STAT3 with mutations in nuclear localization sequence 1 (NLSI), 2 (NLSII), or both (NLSIII). Cells were either left untreated (A), treated with leptomycin B (LMB) (B), or PDGF and LMB (C) for 4 h and were subsequently fractionated into nuclear (N) and cytoplasmic fractions (C) and protein extracts were analyzed by immunoblotting using antibodies specific for STAT3 or tubulin as a marker of cytosolic protein. STAT3-NLSIII did not accumulate in cell nuclei, even following stimulation by PDGF and inhibition of nuclear export by LMB.

Figure S3: Ras-induced RalA activity is STAT3 dependent, but RalA activity is not necessary for Ras-induced transformation. (A) Total cellular protein from STAT3-deficient cells expressing H-RasV12 stably transduced with empty vector (EV) or wild

type STAT3 (WT) were subjected to Ral-BP1 binding assays to measure RalA activation. Total RalA served as a loading control. **(B)** STAT3-deficient cells expressing H-RasV12 stably transduced with empty vector and a constitutively active RalA mutant (EV + Ral72L) or with wild type STAT3 and a dominant negative RalA mutant (WT + Ral28N) were assayed for growth in soft agar. Average colony number was calculated from three biological replicates. Error bars represent SD.

Figure S4: STAT3 localizes to the mitochondria in primary mouse liver, human cancer cells (T24), and non-transformed human breast epithelial cells (MCF10A).

(A) Livers were isolated from wild type C57BL/6 mice 16 h after food restriction, the tissue was separated into cytoplasmic (cyto) and mitochondrial (mito) fractions following mechanical disruption. **(B)** Human bladder carcinoma (T24) cells or breast epithelial (MCF10A) cells were separated into cytoplasmic and mitochondrial fractions. Cellular fractions were assessed for the presence of STAT3 and the purity of fractions were confirmed by using antibodies to Erk1/2 (cytosol) or Bcl-X_L (mitochondria). Data shown are representative of three biological replicates.

Figure S5: Expression of STAT3 and STAT3 mutants in mitochondria of N- and K-Ras-transformed cells. STAT3-deficient N-RasV12- or K-RasV12-expressing cells were stably transduced with empty vector (EV), wild type STAT3 (WT), S727A mutant STAT3 (S/A) or mitochondrially-restricted STAT3 (MTS-STAT3). Total cellular **(A)** and cytoplasmic and mitochondrial protein fractions **(B)** were separated by SDS-PAGE and probed with antibodies specific for STAT3 phosphorylated on S727, total STAT3, or loading controls: tubulin (total protein), Erk (cytosolic protein), and Bcl-X_L (mitochondrial protein).

Figure S6: STAT3 protects cells from mitochondrial poisons but does not alter mitochondrial number or gene expression. **(A)** Equivalent numbers of STAT3-expressing (wild type) or deficient (knockout) H-RasV12-expressing cells were stained with Mitotracker Red and the mean fluorescence intensity measured by flow cytometry to determine the relative mitochondrial mass of the two cell lines. **(B)** Mitochondrial DNA

or (C) RNA was extracted from equivalent numbers of STAT3-expressing (WT) or deficient (KO) H-Ras-expressing cells and the copy number of each gene in the mitochondrial genome and its expression were determined by real-time PCR and RT-PCR, respectively. Data are represented as averages of the ratio of individual mitochondrial genes in STAT3-deficient (KO) to STAT3-expressing (WT) cells, and error bars represent SD of three independent experiments. (D) The relative concentration of ATP was assessed in H-RasV12-expressing wild type (WT) or STAT3-deficient (KO) cells. STAT3-expressing (wild type) or deficient (knockout) H-Ras-expressing cells were treated with Rotenone (E), Antimycin A (F), or Oligomycin (G) at the indicated doses for 24 h. Cell death was measured by trypan blue exclusion assay and the means and standard deviations of three independent experiments are shown.

Figure S7: Mitochondrially-restricted STAT3 is sufficient to maintain H-RasV12-induced solid tumor growth. Fox Chase SCID mice were injected with 10^4 H-RasV12-expressing STAT3-deficient cells (left flank, dashed grey arrow) or H-RasV12-expressing STAT3-deficient cells, which had been reconstituted with a mitochondrially restricted wild type STAT3 using a GFP-expressing vector (right flank, solid black arrow). Mice only grew tumors on the right flanks, which were readily discerned in either the dorsal (A) or ventral view (B), once the skin had been resected. Tumors were resected (C) and confirmed to be H-RasV12-MTS-STAT3 by virtue of bicistronic expression of both GFP and MTS-STAT3 (D). H-RasV12-expressing STAT3-null cells transduced with empty vector failed to grow, while MTS-STAT3-transduced tumors were detected in 5 out of 5 mice.

Figure S8: STAT3 is not required for activity of electron transport chain complexes I, III, and IV. The activities of electron transport chain complexes I (A), III (B), and IV (C) were compared between H-RasV12-expressing wild type (WT) or STAT3-deficient (KO) cells. Activity expressed as the unit activity of individual complexes normalized to citrate synthase activity from equivalent numbers of mitochondria. Results are means and SD from 3 replicates. Error bars indicate SD.

Supplemental References

- S1. K. Schlessinger, D. E. Levy, *Cancer Res.* **65**, 5828 (2005).
- S2. M. Chatterjee *et al.*, *Blood* **104**, 3712 (2004).
- S3. Y. Wang, W. Zhu, D. E. Levy, *Methods* **39**, 356 (2006).
- S4. A. J. Janssen *et al.*, *Clin Chem* **53**, 729 (2007).
- S5. E. J. Lesnefsky *et al.*, *Am J Physiol* **273**, H1544 (1997).
- S6. S. Krahenbuhl, M. Chang, E. P. Brass, C. L. Hoppel, *J. Biol. Chem.* **266**, 20998 (1991).
- S7. C. Godinot, D. C. Gautheron, Y. Galante, Y. Hatefi, *J. Biol. Chem.* **256**, 6776 (1981).
- S8. M. G. Stanton, *Anal. Biochem.* **22**, 27 (1968).
- S9. P. A. Srere, *Meth. Enzymol.* **13**, 3 (1969).
- S10. N. Mitin, K. L. Rossman, C. J. Der, *Curr. Biol.* **15**, R563 (2005).
- S11. N. M. Hamad *et al.*, *Genes Dev.* **16**, 2045 (2002).